Comparison of Implant Body Designs and Threaded Designs of Dental Implants: A 3-dimensional Finite Element Analysis

Heng-Li Huang, MS, PhD[1]/Chin-Han Chang, MS, PhD[2]/Jui-Ting Hsu, MS[3]/
Alison M. Fallgatter, DDS, MS[4]/Ching-Chang Ko, DDS, PhD[5]

Purpose: *Stress analysis was performed for various implant designs using 3-dimensional finite element analysis approaches.* ***Materials and Methods:*** *Six implant designs were included: 3 parallel-sided implants (no thread, triangular thread, and squared thread), 2 stepped configurations (non-thread and triangular thread), and a tapered body of implant with squared thread. All threads had spiral characteristics. The mandibular model was constructed from computed tomographic (CT) images of a human mandible, and the material properties were anisotropic (different in different directions). A 100-N oblique force was applied at a 45-degree angle to the long axis of the implants at the buccal cusp as the loading condition.* ***Results:*** *Compared with cylindric implants, threaded implants (either triangular or squared) demonstrated increased peak stress at the crestal bone. The bone stress of stepped implants was decreased in the cortical region but was increased in the trabecular region. However, both threaded and stepped designs showed decreased interfacial stresses of bone near the valleys of the threaded and stepped areas. The tapered design decreased stresses by up to 32% in the cortical region and 17% in the trabecular region.* ***Conclusions:*** *Although threaded implants could not decrease the peak stress at the crestal bone, both threaded and stepped designs show an ability to dissipate the interfacial stresses of bone. The use of tapered implants could reduce peak stress in both cortical and trabecular bone.* Int J Oral Maxillofac Implants 2007;22:551–562

Key words: *finite element analysis, implant designs, threads*

Various dental implant designs have been advocated to reduce bone loss of crestal regions and osseointegrated interfaces. Some of these designs may decrease biomechanical loading and thus decrease bone loss.[1,2] Overloading may induce microdamage to the bone, which can trigger osteoclastogenesis.[3] Sequentially, epithelial tissues, connective tissues, and microorganisms can migrate into the defective area and cause severe bone loss,[4] which decreases the implant's bone support and increases the risk of implant failure.[5,6]

There are 3 major design concepts: the threaded implant body, the stepped implant body, and the tapered implant body. These designs have been proposed to improve the clinical and biomechanical behavior of oral implants.[1,2,7,8] The use of the threaded implant may increase the contact area between the implant and bone, decrease implant mobility at the time of implant placement, and help dissipate interfacial stresses.[7,8] Likewise, it has been suggested that the stepped implant creates favorable load distribution by mimicking the natural root form.[1] Another design concept is to redirect stresses using a tapered implant body. This type of implant has shown a reasonably good survival rate,[9] perhaps because it directs stress away from the crestal cortical bone while transferring it to the trabecular bone.[2] In addition, the use of tapered implants and square-threaded implants reduces the time required for implant placement, because fewer threads twist through bone.

[1]Assistant Professor, School of Dentistry, China Medical University, Taichung, Taiwan.
[2]Professor, Institute of Biomedical Engineering, National Cheng Kung University, Tainan, Taiwan.
[3]Postdoctoral Researcher, Institute of Biomedical Engineering, National Cheng Kung University, Tainan, Taiwan.
[4]Graduate Student, Department of Diagnostic and Biological Sciences, University of Minnesota, Minneapolis, Minnesota.
[5]Associate Professor, Department of Orthodontics, University of North Carolina, Chapel Hill, North Carolina.

Correspondence to: Dr Ching-Chang Ko, Department of Orthodontics, University of North Carolina, CB# 7450, Chapel Hill, NC 27599-7450. Fax: +919 843 8864. E-mail: koc@dentistry.unc.edu

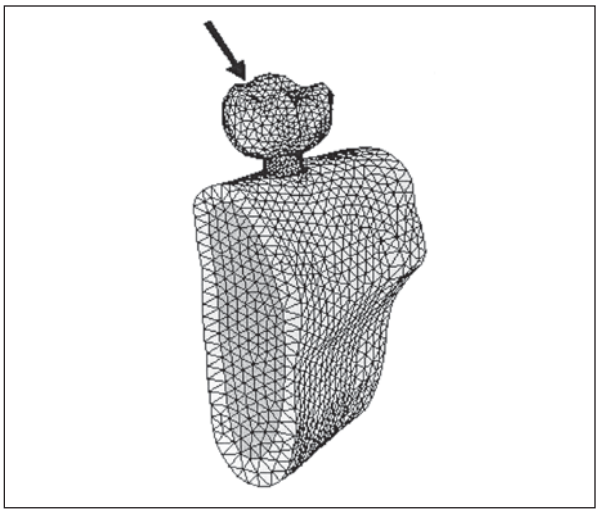

Fig 1 The finite element model included the crown, the implant, and the posterior mandible. The model contains about 42,500 elements and 61,300 nodes. The 100-N oblique load was applied to the buccal cusp of the crown. The boundary condition was set to fix the bottom surface of the mandibular section.

Each of these 3 designs has certain advantages. However, there is no general consensus regarding which design could most improve biomechanical performance by reducing stress magnitudes in cortical and trabecular bone and even at the bone-implant interface. Due to the complicated 3-dimensional (3D) structure of these implant designs, no study has shown whether bone stresses can be more uniformly distributed using the stepped or tapered design. Three-dimensional finite element (FE) analysis has been widely used to predict stress/strain on bone and implants. However, in previous FE analyses, threads were constructed based on discontinuous and axisymmetric assumptions.[10,11] According to the appendix of this study, the models neglected the spiral characteristic and thus may have over- or underestimated stress in the peri-implant bone.

In the present investigation, 3D FE models of various implants in a human mandible were developed. The biomechanical effects of the use of *(1)* a threaded implant body, *(2)* a stepped implant body, and *(3)* a tapered implant body were investigated.

MATERIALS AND METHODS

Solid models of a mandibular segment, a porcelain crown, and dental implants developed using computer-aided design (CAD) were used to construct implant-bone FE models (Fig 1). The posterior mandible (from distal to the second premolar to mesial to the second molar) was harvested from a dry human skull, and frontal sections of computerized tomographic (CT) images were obtained (1 mm interval between images). From each CT image, material boundaries were delineated by an in-house imaging program. This program employed various thresholds in CT number and searched for maximum gradient values of the CT number, which were used to detect the boundary pixels between different materials.[12] A depth-first search algorithm was then used to find the nearest boundary pixels to renumber the pixels and construct the contour of each material. The coordinates of points forming the contour lines were then imported into the Fe software ANSYS (Swanson Analysis, Huston, PA) to generate a solid 3D model of the mandible.

A CT scan of an implant-supported acrylic resin crown from the first molar area was obtained. A 3D solid model of the crown was created by the same procedure used for the mandible. The dimensions of the mandibular bone model were about 36 mm high, 20 mm long mesiodistally, 5.5 mm wide buccolingually at the crestal bone of the premolar site, and 7.3 mm wide buccolingually at the crestal bone of the molar site.

The implant model was constructed using the CAD system (Pro-Engineering, PTC, New York, NY). For the threaded implant, the helical sweep function was used to generate the geometry of spiral screws. Six implant designs were studied:

- Nonthreaded cylinder
- Triangular thread with a straight implant body
- Square thread with a straight implant body
- Nonthreaded stepped implant
- Triangular thread with a stepped implant body
- Squared thread with a tapered implant body

The CAD file for the implant models was saved as an IGES file and imported to ANSYS to generate solid models of implants. After all models were combined by overlap of the Boolean operation, 10-node tetrahedral p-elements (ANSYS solid 148) were used to construct the finite element models. Except for the stepped implants (4.25 mm in first step of diameter), the implants were all the standard 3.75 mm in diameter. The length of all implants was 11.5 mm. Components such as hexagonal abutments and abutment screws were omitted. The meshed models and the detail dimensions of 6 implants are shown in Figs 2 and 3.

The material properties of cortical and trabecular bone were modeled as being transversely isotropic and linearly elastic,[13] which describes an anisotropic material (ie, a material with different properties in different directions). For the cortical bone, the material properties of the buccal and lingual directions were isotropic along the axis of the mesiodistal

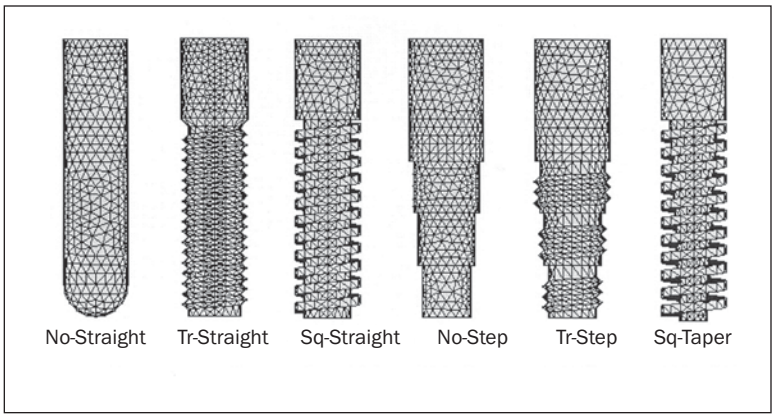

Fig 2 The FE models of the 6 implant designs studied. In order to label these models, two sets of symbols were used. The first part of the design name denotes the shape of the thread: "No" for non-thread, "Tr" for triangular thread, and "Sq" for squared thread. The second part denotes shape of the implant body: "Straight" for straight implant body, "Step" for stepped implant body, and "Taper" for tapered implant body.

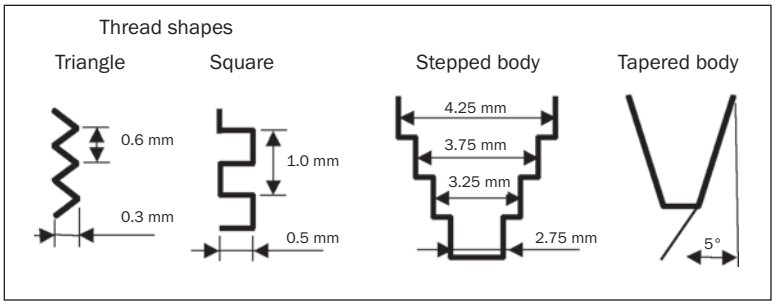

Fig 3 The dimensions of the threads, the stepped implant body, and the tapered implant body.

Table 1 Material Properties of the FE Model

Material	Young's modulus E (MPa)	Poisson's ratio (ν)	Shear modulus G (MPa)
Cortical bone	E_x 12,600	ν_{xy} 0.300	
		ν_{yz} 0.253	G_{xy} 4,850
	E_y 12,600	ν_{xz} 0.253	
		ν_{yx} 0.300	G_{yz} 5,700
	E_z 19,400	ν_{zy} 0.390	
		ν_{zx} 0.390	G_{xz} 5,700
Trabecular bone	E_x 1,148	ν_{xy} 0.055	
		ν_{yz} 0.010	G_{xy} 68
	E_y 210	ν_{xz} 0.322	
		ν_{yx} 0.010	G_{yz} 68
	E_z 1,148	ν_{zy} 0.055	
		ν_{zx} 0.322	G_{xz} 434
Titanium	110,000	0.350	
Porcelain	70,000	0.190	

The vectors of x, y, and z indicate the buccolingual, inferosuperior, and mesiodistal directions, respectively.

direction; likewise, the material properties of 2 directions on the anatomic transverse plane of trabecular bone were isotropic in the inferosuperior direction. The materials of the implant and prosthetic crown were assumed to be isotropic and linearly elastic.[14,15] All material properties are listed in Table 1. The buccal oblique force (100 N) was applied at a 45-degree angle to the long axis of the implant on the buccal cusp as the loading condition (Fig 1). The bottom surface of mandibular bone was constrained in the x, y, and z directions (displacement = 0) as the boundary condition. The bone-implant interface and crown-implant interface were rigidly bonded in all models.

The highest maximum and minimum principal stresses of bone were used for the comparison. In addition, the interfacial stresses in bone along the implants' buccal and lingual surfaces from the alveolar crest to the apex of the implant were analyzed and compared among the 6 models. The p-element method in ANSYS was used for the convergence tests, and by this method the polynomial level (p-level) of the element shape functions was manipu-

lated. Therefore, in the models the degree of the polynomial level (p-level) of the element shape functions was adjusted from 2 (the initial value) to 8 until the convergence criteria were achieved. Change in the global strain energy was required to be less than 5% at a p-level of 4 at convergence.

RESULTS

Figures 4a and 4b show the von Mises stress distributions on cortical and trabecular bone of the 6 FE models. Table 2 shows the highest maximum principal (tensile) and minimum principal (compressive) stresses of the cortical and trabecular bone for the 6 models. In general, the highest stresses of cortical bone were located at the crestal cortical bone around the implant, which corresponded with the clinical finding of crestal bone loss.[3] In addition, stresses of the endosteal cortical bone were high in cylindric (No-Straight) and stepped (No-Step and Tr-Step) implants. For the trabecular bone, the stress was concentrated near the endosteal trabecular bone, the tip of the thread, the apex of the implant, and the stepped areas where the diameter of the implant changed.

Effect of Thread

Regarding the models of straight implants, peak tensile stress in cortical bone was 42% higher for the Tr-Straight model than for the No-Straight model, although peak tensile stress in trabecular bone for the 2 models was nearly the same. Likewise, peak tensile stress in cortical bone was 73% higher for the Sq-Straight model than for the No-Straight model; in trabecular bone, it was 71% higher. Peak compressive stress was about 34% greater in cortical bone and 36% greater in trabecular bone for Tr-Straight and Sq-Straight compared to No-Straight.

Regarding the models of stepped implants, peak tensile stress was 5% greater in the Tr-Step implant than the No-Step implant in cortical bone and 70% greater in trabecular bone. There was no difference in peak compressive stress in cortical bone between the Tr-Step and No-Step models. However, compressive stress in trabecular bone was 20% lower in the Tr-Step model than in the No-Step model.

Effect of Step Design

Compared with the No-Straight model, the peak tensile stress of the No-Step model was decreased by 11% in cortical bone; however, peak tensile stress was identical in trabecular bone for the 2 models. Likewise, the peak compressive stress of the No-Step model was decreased by 17% in the cortical bone compared with the No-Straight model but was increased by 36% in the trabecular bone.

Effect of Tapered Design

Compared with the Sq-Straight model, the peak tensile stress of the Sq-Taper model was decreased by 32% and 17% in cortical and trabecular bone, respectively; likewise, the peak compressive stress of Sq-Taper model was decreased by 18% and 10% in cortical and trabecular bone, respectively, compared to the Sq-Straight model.

Anatomic Effect on Interfacial Stresses Profile

Interfacial stresses of bone along buccal and lingual surfaces of the implants were plotted in Figs 5 to 8 from the peak of the alveolar crest (0%) to the apex of the implant (100%). Results needing attention were the stress curves of the threaded and stepped designs in trabecular bone. In these situations, lower bone stresses were demonstrated near the valleys of the threaded and stepped areas. The tapered design showed the least stress at the alveolar crest among the 6 models.

Interfacial Stresses in Cortical Bone. The stress patterns of the Tr-Straight and Sq-Straight models along the buccal surfaces of the implants were similar to that of the No-Straight model; however, along the lingual surface of the implant, the Tr-Straight and Sq-Straight models showed lower stress in the endosteal cortical region than the No-Straight model. For the stepped design, Model No-Step showed an identical stress pattern to Model No-Straight. Stress in the endosteal cortical region was relatively low in the Tr-Step model compared with the No-Step model. Nevertheless, the tapered body design of the Sq-Taper model demonstrated the ability to decrease stress in the alveolar crestal area.

Interfacial Stresses in the Trabecular Bone. The interfacial bone stresses varied among the No-Straight, Tr-Straight, and Sq-Straight models. Both threaded models (Tr-Straight and Sq-Straight) showed low stress in the valleys of the threads as compared to the No-Straight model. The stepped implants (No-Step and Tr-Step) also demonstrated lower stresses at the stepped areas as compared with the cylindric implant (No-Straight). The Tr-Step implant was also associated with low stresses in the valley areas. The stress patterns of the tapered (Model Sq-Taper) and nontapered body designs (Model Sq-Straight) were almost identical.

Fig 4a The von Mises stress distribution in the buccolingual cross section of cortical shell.

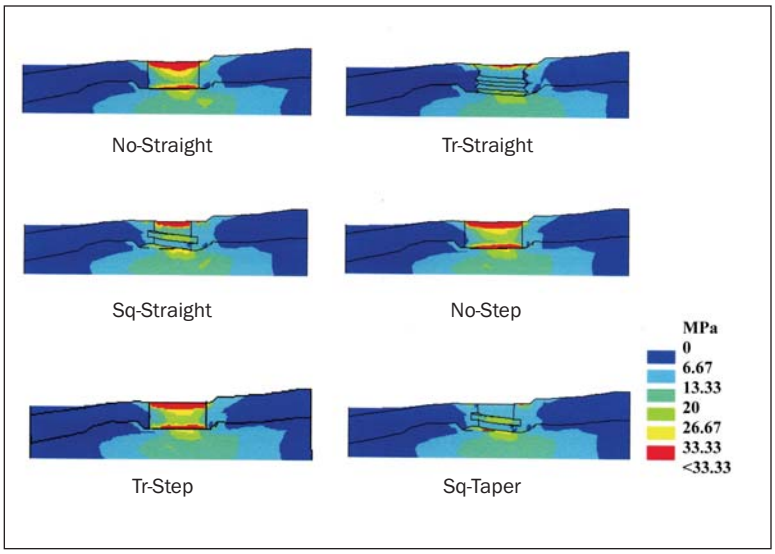

Fig 4b The von Mises stress distribution in the buccolingual cross section of trabecular bone.

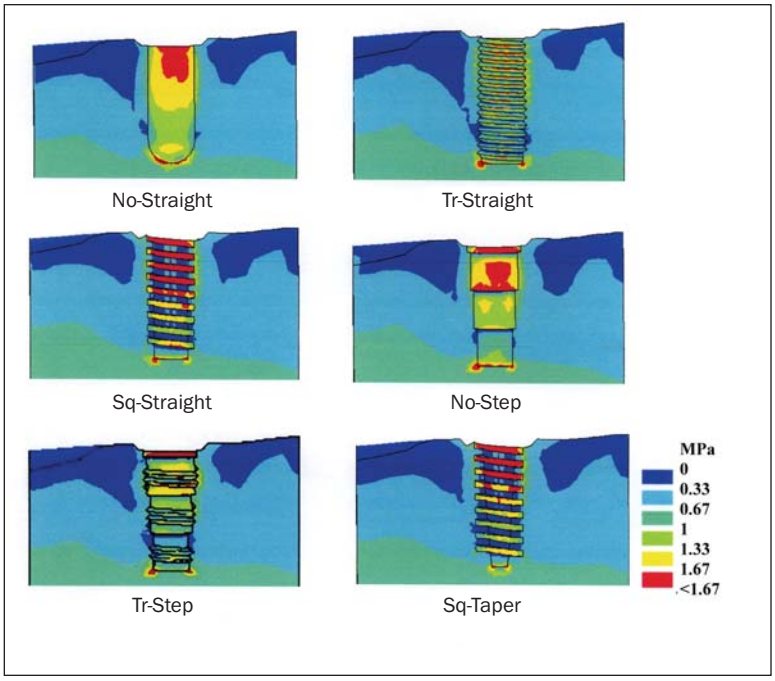

Table 2 The Highest Maximum and Minimum Principal Stress (MPa) in Cortical and Trabecular Bone Around the Implant

Model	No-Straight	Tr-Straight	Sq-Straight	No-Step	Tr-Step	Sq-Taper
Cortical bone						
P_{max}	122.8	174.8	212.5	109.1	114.9	144.1
P_{min}	−165.5	−222.0	−221.8	−136.8	−136.8	−182.8
Trabecular bone						
P_{max}	3.1	3.0	5.3	3.0	5.1	4.4
P_{min}	−2.2	−3.0	−2.9	−3.0	−2.4	−2.6

P_{max} = maximum principal stress; P_{min} = minimum principal stress.

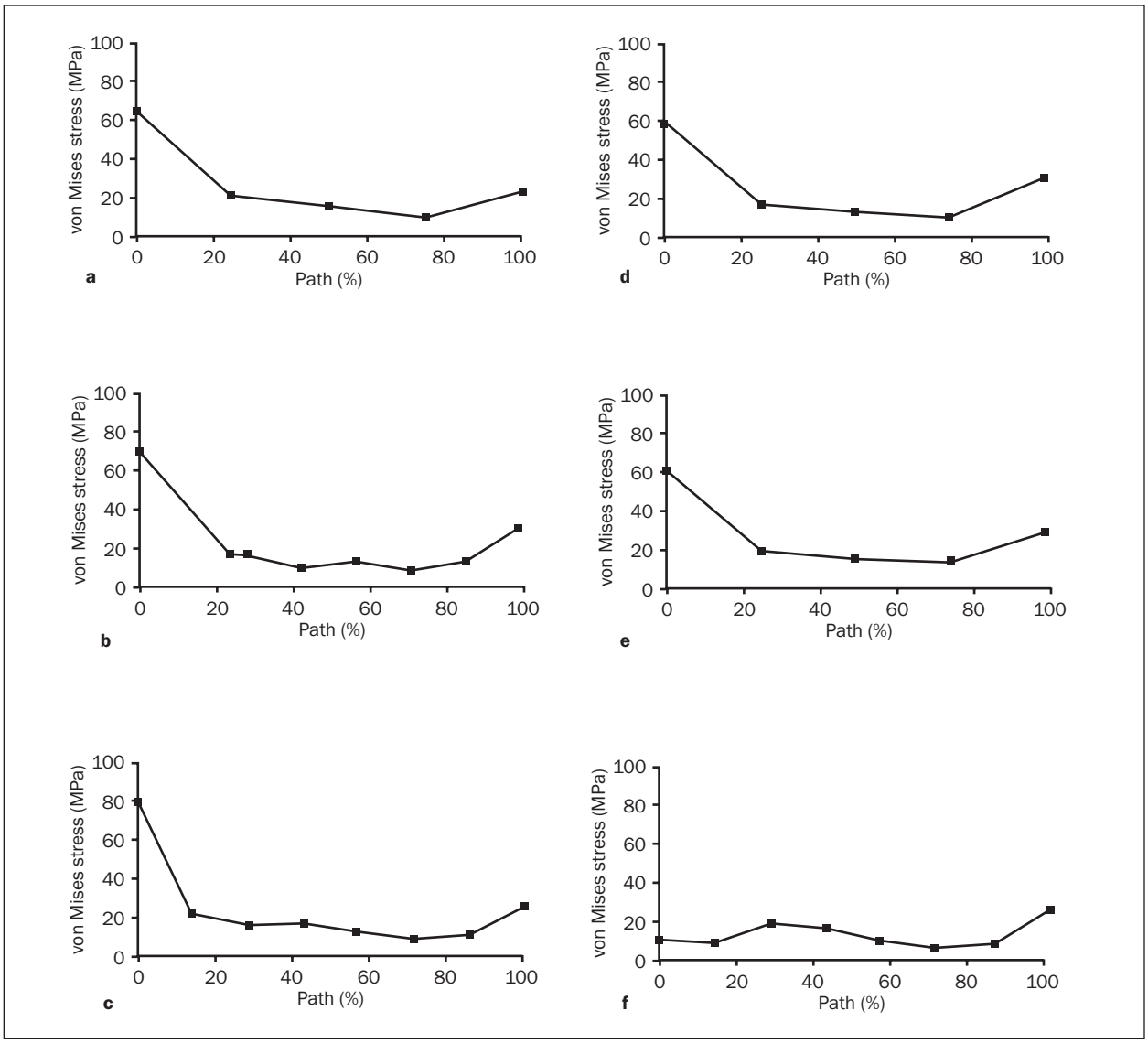

Fig 5 The implant-bone interfacial stresses in cortical bone along the buccal wall for the *(a)* No-Straight, *(b)* Tr-Straight, *(c)* Sq-Straight, *(d)* No-Step, *(e)* Tr-Step, and *(f)* Sq-Taper models.

DISCUSSION

In this study, 3D features of dental implant-bone models, including various thread shapes, body types, and bone types, have been investigated using computational biomechanical approaches. FE modeling of dental implants often uses simplified nonspiral (axisymmetric rings) threads.[10,11] The nonspiral approach, though less complex in construction, yields errors in prediction (Appendix). The current study combined models of spiral threaded implants with models with natural structures and the anisotropic properties of alveolar bone. It was found that the predicted peak stress varied with location in the alveolar ridge. The approach accounted for actual implant configuration and anatomic structure, allowing more accurate stress prediction.

All models revealed a peak stress localized at the crestal region of cortical bone, concurring with previously reported analyses.[11,13,16,17] Although the occlusal forces applied in all 6 models were 100 N, lower than the measured data of 129 N by Morneburg et al,[18] the peak tensile and compressive stresses were beyond the ultimate tensile (100 MPa) and compressive (173 MPa) strength of cortical bone.[19] These high stresses could cause mechanical overloading of bone and result in alveolar bone loss. These peak stresses on cortical bone were highest in the threaded implants. Nevertheless, the results of

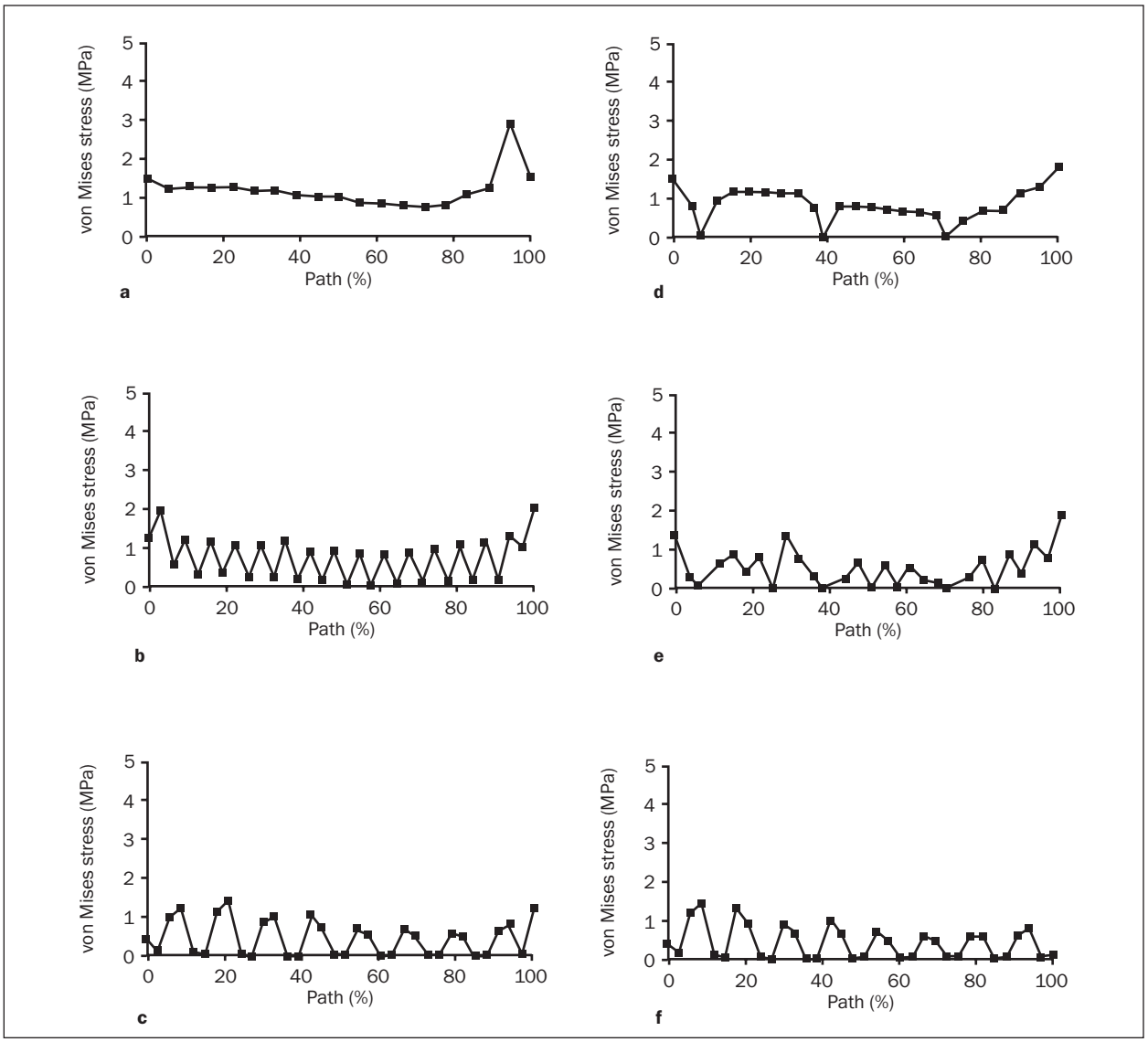

Fig 6 The implant-bone interfacial stresses in trabecular bone along the buccal wall for the *(a)* No-Straight, *(b)* Tr-Straight, *(c)* Sq-Straight, *(d)* No-Step, *(e)* Tr-Step, and *(f)* Sq-Taper models.

this study did not signify that using threaded designs would increase implant failure rates. According to the results of interfacial stresses of bone, threaded designs lowered the stresses near the valley of the thread. This is consistent with a prior study[6] that claimed that a threaded design could dissipate interfacial stresses. Furthermore, the clinical advantages of improved stability[20,21] and stress-induced bone formation[22] may also affect or extend the survival rate of implants with a threaded design.[23,24] Further research is needed on these potential benefits of a threaded implant design.

Both threaded and stepped designs showed a wavy interfacial stress pattern along the implants' surface in trabecular bone, while the cylindric implant revealed 1 large high-stress area. Recent studies have shown a similar trend with FE models of the spiral threaded implant[25,26] and stepped implant.[27] These studies revealed that threaded and stepped characteristics dissipated the stress transfer pathway from a single high-stress area into numerous disconnected areas of bone near the threads' tips and stepped areas. However, the reason for this dissipation is unknown. This study demonstrated that the reason for this dissipation may be 2 mechanical factors—the stress concentration yielded by geometric discontinuity and the stress shielding effect.[28] First, the geometric discontinuity of

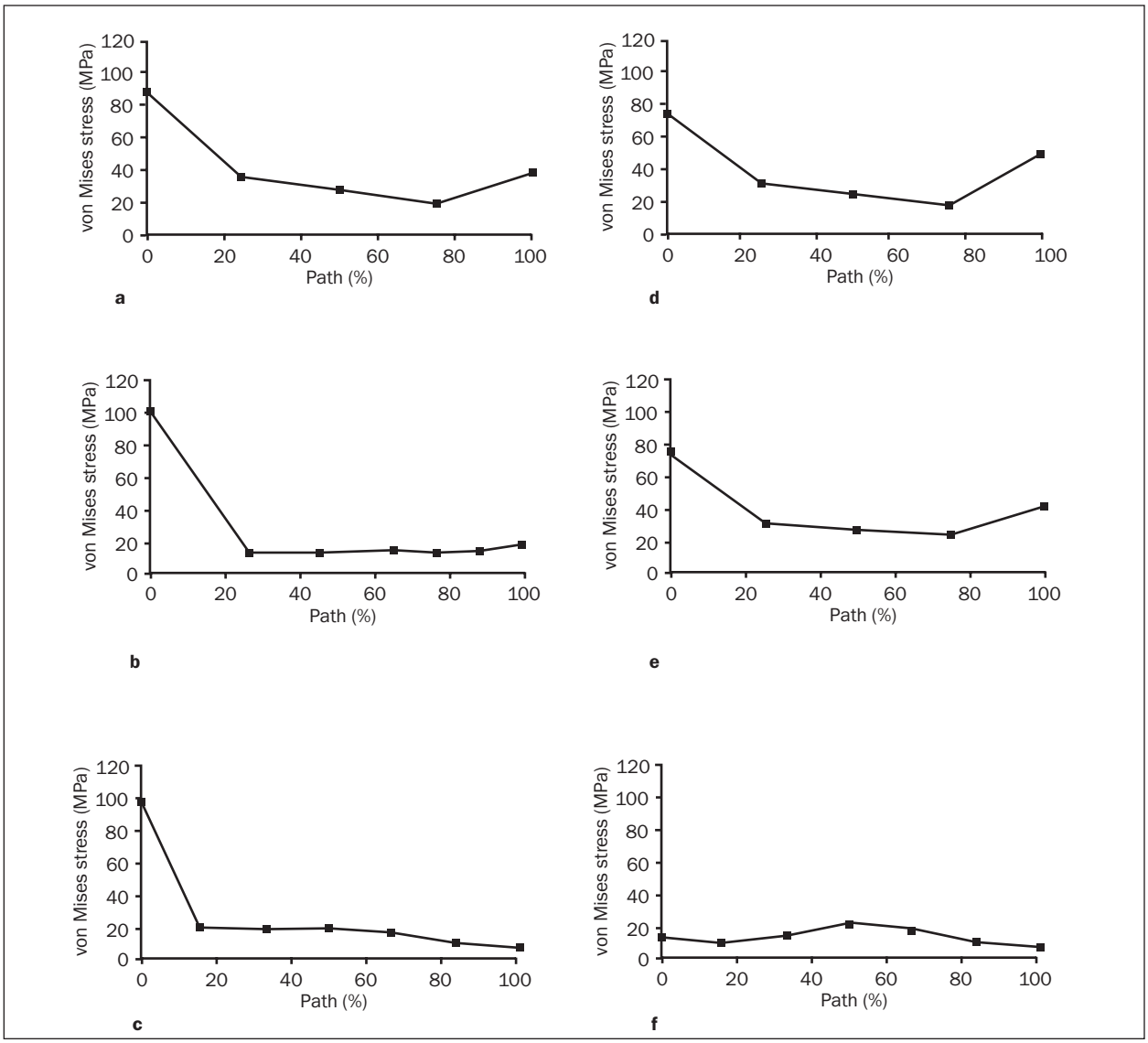

Fig 7 The implant-bone interfacial stresses in cortical bone along the lingual wall for the *(a)* No-Straight, *(b)* Tr-Straight, *(c)* Sq-Straight, *(d)* No-Step, *(e)* Tr-Step, and *(f)* Sq-Taper models.

threaded and stepped designs resulted in high stresses at the valley between pitches and stepped areas (Fig 9). This circumstance could be explained by the flexure formula and the following stress concentration factor[29]:

$$\sigma_{sur} = K \cdot MC/I$$

where $I = \pi C^4/4$ and where K is the stress concentration factor, M is the bending moment, C is a distance from the surface to central axis of the implant and I is the moment of inertia of circular cross. In this study, only M was constant; the interfacial stress of the implant varied as the values of K, C, and I varied. For the uniform surface of the cylindric implant, K was equal to 1 and could be ignored. However, for the threaded and stepped designs, the geometric discontinuity increased the value of K and resulted in higher stresses at the valley between pitches and stepped areas. In addition, in the valleys of the threads and inferior stepped areas, the radii were smaller than those on the tip of thread and the superior stepped areas. Thus, stresses increased nonlinearly on the implant surface. This is also known as the stress shielding effect. High stress was primarily transferred through the implant surface of the valley of thread and the stepped areas, reducing the stresses in bone near the interface. These lower interfacial stresses in bone may improve

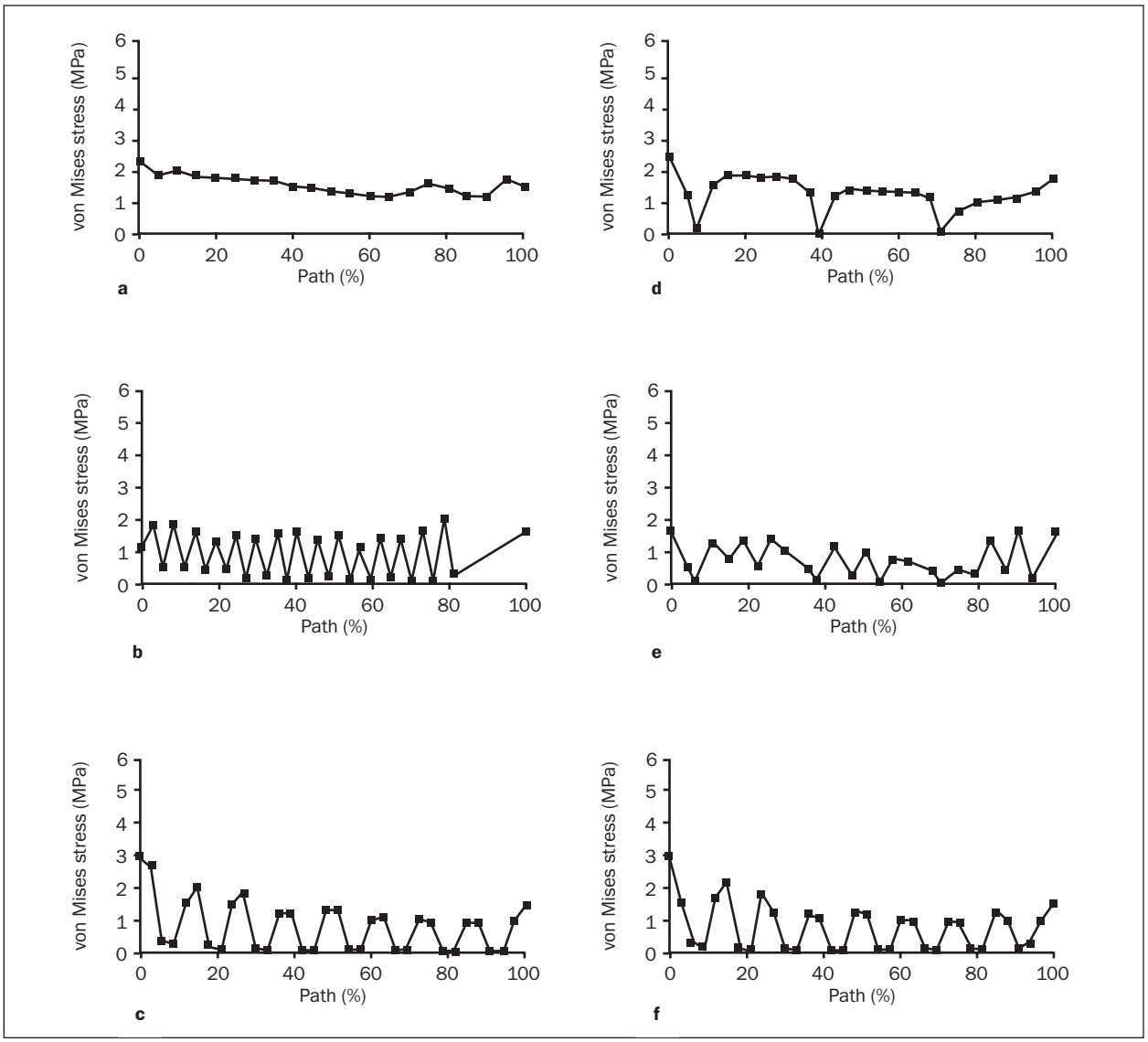

Fig 8 The implant-bone interfacial stresses in trabecular bone along the lingual wall for the *(a)* No-Straight, *(b)* Tr-Straight, *(c)* Sq-Straight, *(d)* No-Step, *(e)* Tr-Step, and *(f)* Sq-Taper models.

Fig 9 The localized stress pattern of *(left)* a triangular thread implant and *(right)* a stepped implant.

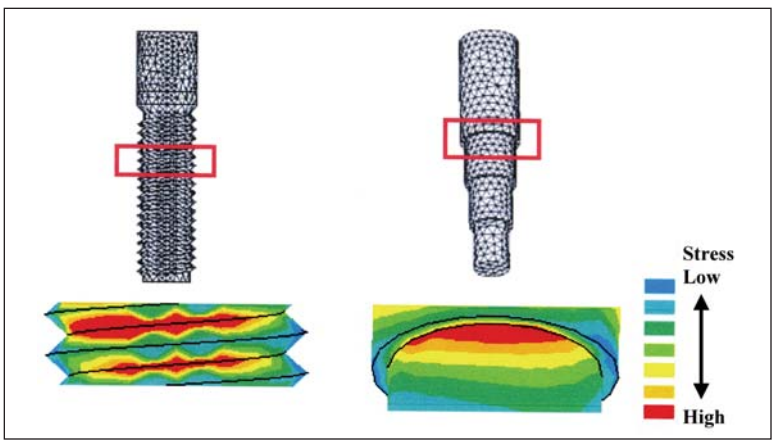

osseointegration and benefit the threaded implant with greater bone-implant contact.[30] Additionally, the square thread showed larger areas of low interfacial stresses near the tips of the implant in trabecular bone compared to the triangle thread.

The root-analog design was suggested because it mimics the shape of natural roots, which implies favorable stress dissipation in the surrounding bone.[1] However, in the current study, the stress of the stepped implant was different in cortical and trabecular bone. As compared to the cylindric implant, only the peak stress of cortical bone was decreased in the stepped implants. This is because the diameter of the first step of the stepped implant was 4.25 mm, which is larger than the standard size (3.75 mm in diameter) of the cylindric implant. This larger diameter increased the bone-implant contact area and lowered the peak stress in the crestal cortical region. Nevertheless, the stepped implant did not decrease the peak stress of trabecular bone because the contact area in trabecular bone was not increased. Furthermore, adding threads on the stepped cylinder showed the advantage of decreasing the interfacial bone stresses near the valley of the thread.

The tapered implant body (Model Sq-Taper) decreased stresses in both cortical and trabecular bone compared to the Sq-Straight design. The tapered body was adopted from the Ankylos implant system (Friadent, Mannheim, Germany), which was aimed to release stress in cortical bone and transfer more stress into trabecular bone. In a photoelastic experiment, Morris et al[2] found stress values decreased in cortical bone but increased in trabecular bone, which supported the original design concept. However, in this experiment, only 1 photoelastic material was used to construct the bone structures. This means that cortical bone and trabecular bone were simulated by the same photoelastic material. The current study simulated cortical and trabecular bone by using different materials. It also accounted for natural 3D geometry of the implant-bone complex. The results further demonstrated that the tapered body reduced stresses not only in cortical bone but also in trabecular bone. The increased depth of the thread in the tapered body design profoundly increased the interfacial area for bone-implant contact, which may be attributed to this biomechanical effect.

There are limitations associated with this current simulation. First, this study only analyzed a bonded status in bone-implant interface. For the investigation of interfacial stresses, the nonbonded situation is another important consideration. Several studies have demonstrated that the absence of interfacial bonding would influence stress and strain patterns in bone near the interface[4] and, furthermore, that the nonbonded interface would more than double stresses and strains of bone compared to the bonded interface.[4,31,32] In addition, viscoelastic material properties were not included in bone models. Both the effects of the nonbonded interface and the viscoelasticity of the 6 implants need to be investigated further. Second, biologic variations might lead a significant variation in stress/strain stimuli. However, with current computational power, it is not feasible to include these variations in an analysis. Confirmative information for the implant designs in this study also requires further experimental evidence and more clinical trials. Nevertheless, from the biomechanical standpoint, both threading and body design are important factors affecting stress in the surrounding tissue and implant osseointegration. Although the threaded design showed no ability to decrease the peak stress in the crestal bone region, both it and the stepped design were able to dissipate the interfacial bone stresses. The tapered body design appeared more able to reduce stress in the crestal cortical and endosteal trabecular bone than the other designs.

CONCLUSIONS

Within the limitation of this study, the results demonstrate the following:

1. Although the inclusion of thread in an implant design increases contact area, it does not decrease the peak bone stress. However, the thread does depress the interfacial stresses of bone.
2. A stepped implant reduces the peak stress of cortical bone. In addition, stepped implants lower the interfacial bone stresses at stepped areas.
3. Use of a tapered threaded body design could decrease bone stresses because of the extension of contact area.

ACKNOWLEDGMENTS

This research was supported by grant NSC 95-2218-E-039-001 from National Science Council, Taiwan (Republic of China), the Minnesota Dental Research Center for Biomaterials and Biomechanics, and the US National Institutes of Health/National Institute of Dental and Craniofacial Research (NIH/NIDCR R21DE015410).

APPENDIX: SPIRAL VERSUS NONSPIRAL MODELS

There is a large body of biomechanical research using the concentric circles (nonspiral) to imitate spiral threads of dental implants. From the standpoint of engineering, the previous nonspiral threaded implant model does not represent actual implant design and certainly cannot provide accurate biomechanical information. This appendix provides supplemental information to compare differences between spiral and nonspiral implants.

Finite element analyses of the nonspiral threaded implant and spiral threaded implant were performed (Fig A1). The method used to construct these models was the same as that described in the Materials and Methods section of the present study. The models used the same anisotropic material properties (Table 1), loading conditions, and boundary conditions. Peak stresses and stress distribution patterns were compared.

Table A1 shows the highest maximum principal (tensile) and minimum principal (compressive) stresses on the cortical and trabecular bone for the nonspiral and spiral threaded implants. The nonspiral threaded implant was lower (up to 14.1%) in cortical bone and was higher (up to 50.8%) in trabecular bone as compared with the spiral threaded implant. In addition, the nonspiral threaded implant demonstrated an increased total area of high stress (with the same contour ranges) at crestal cortical bone. An area of profound stress concentration was found in trabecular bone near the endosteal cortex in conjunction to the third and fifth threads (Fig A2).

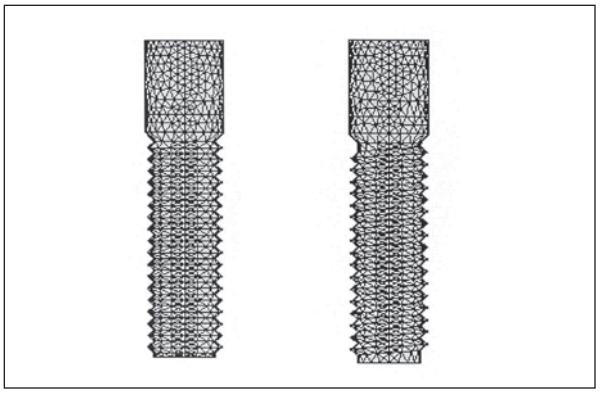

Fig A1 FE models of *(left)* an implant with nonspiral threads and *(right)* an implant with spiral threads.

Table A1 The Highest Maximum (Tensile) and Minimum (Compressive) Principal Stress Value (MPa) in Cortical and Trabecular Bone for Nonspiral and Spiral Threaded Implants

	Cortical bone		Trabecular bone	
	P_{max}	P_{min}	P_{max}	P_{min}
Nonspiral threads	164.4	−194.6	4.6	−6.1
Spiral threads	174.8	−222.0	3.0	−3.0

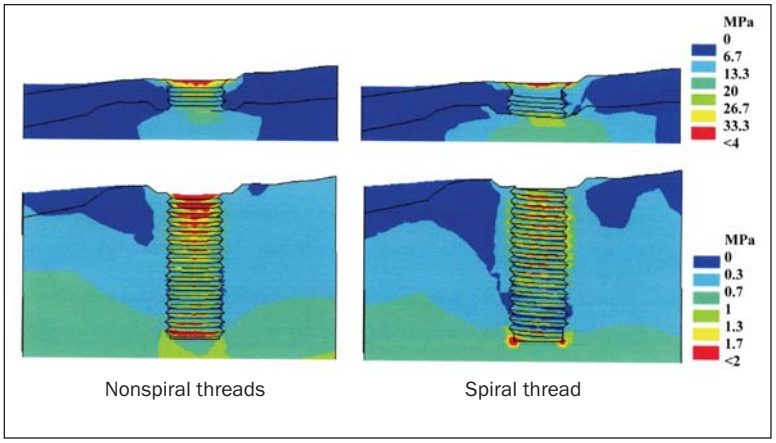

Fig A2 von Mises stress distribution for the models of nonspiral and spiral threaded implants. Buccolingual cross sections are shown *(top)* in the cortical shell and (bottom) in trabecular bone.

REFERENCES

1. Maiorana C, Santoro F. Maxillary and mandibular bone reconstruction with hip grafts and implants using Frialit-2 implants. Int J Periodontics Restorative Dent 2002;22:221–229.
2. Morris HF, Ochi S, Crum P, Orenstein IH, Winkler S. AICRG, part I: A 6-year multicentered, multidisciplinary clinical study of a new and innovative implant design. J Oral Implantol 2004;30: 125–133.
3. Hansson S. A conical implant-abutment interface at the level of the marginal bone improves the distribution of stresses in the supporting bone: An axisymmetric finite element analysis. Clin Oral Implants Res 2003;14:286–293.
4. Donath K, Hassell T, Jovanovic S, Richter J. Peri-implant pathology. In: Klaus HR, Herbert EW (eds). Color Atlas of Dental Medicine-Implantology. New York: Thieme Medical, 1995:318–319.
5. Rangert B, Krogh PHJ, Langer B, Van Roekel. Bending overload and implant fracture: A retrospective clinical analysis. Int J Oral Maxillofac Implants 1995;10:326–334 [erratum 1996;11:575].
6. Brunski JB. In vivo bone response to biomechanical loading at the bone/dental-implant interface. Adv Dent Res 1999;13: 99–119.
7. Hansson S. The implant neck: Smooth or provided with retention elements. A biomechanical approach. Clin Oral Implants Res 1999;10:394–405.
8. Sykaras R, Iacopino AM, Marker VA, Triplett RG, Woody RD. Implant Materials, designs, and surface topographies: Their effect on osseointegration. A literature review. Int J Oral Maxillofac Implants 2000;15:675–690.
9. Eckert SE, Choi YG, Sanchez AR, Koka S. Comparison of dental implant systems: Quality of clinical evidence and prediction of 5-year survival. Int J Oral Maxillofac Implants 2005;20:406–415.
10. Tada S, Stegaroiu R, Kitamura E, Miyakawa O, Kusakari H. Influence of implant design and bone quality on stress/strain distribution in bone around implants: A 3-dimensional finite element analysis. Int J Oral Maxillofac Implants 2003;18:357–368.
11. Akca K, Cehreli MC, Iplikcioglu H. Evaluation of the mechanical characteristics of the implant-abutment complex of a reduced-diameter Morse-taper implant. A nonlinear finite element stress analysis. Clin Oral Implants Res 2003;14:444–454.
12. Chang CH. Computer Aided Analysis of Femoral Stem Prosthesis [thesis]. Houston, TX: Rice University, 1990.
13. O'Mahony AM, Williams JL, Spencer P. Anisotropic elasticity of cortical and concellous bone in the posterior mandible increases peri-implant stress and strain under oblique loading. Clin Oral Implants Res 2001;12:648–657.
14. Sertgoz A, Guvener S. Finite element analysis of the effect of cantilever and implant length on stress distribution in an implant-supported fixed prosthesis. J Prosthet Dent 1996; 76:165-169.
15. Ciftci Y, Canay S. The effect of veneering materials on stress distribution in implant-supported fixed prosthetic restorations. Int J Oral Maxillofac Implants 2000;15:571–582.
16. Akca K, Iplikciogiu H. Finite element stress analysis of the influence of staggered versus straight placement of dental implants. Int J Oral Maxillofac Implants 2001;16:722–730.
17. Eskitascioglu G, Usumez A, Sevimay M, Soykan E, Unsal E. The influence of occlusal loading location on stresses transferred to implant-supported prostheses and supporting bone: A three-dimensional finite element study. J Prosthet Dent 2004; 91:144–150.
18. Morneburg TR, Proschel PA. Measurement of masticatory forces and implant loads: A methodologic clinical study. Int J Prosthodont 2002;15:20–27.
19. Reilly DT, Burstein AH. The elastic and ultimate properties of compact bone tissue. J Biomech 1975;8:393–405.
20. Ivanoff CJ, Sennerby L, Johansson C, Rangert B, Lekholm U. Influence of implant diameters on the integration of screw implants. An experimental study in rabbits. Int J Oral Maxillofac Surg 1997;26:141–148.
21. Simunek A, Vokurkova J, Kopecka D, et al. Evaluation of stability of titanium and hydroxyapatite-coated osseointegrated dental implants: A pilot study. Clin Oral Implants Res 2002;13: 75–79.
22. Ko CC, Douglas WH, DeLong R, et al. Effects of implant healing time on crestal bone loss of a controlled-load dental implant. J Dent Res 2003;82:585–591.
23. Adell R, Lekholm U, Rockler B, Brånemark P-I. A 15-year study of osseointegrated implants in the treatment of the edentulous jaw. Int J Oral Surg 1981;10:387–416.
24. Ekelund JA, Lindquist LW, Carlsson GE, Jemt T. Implant treatment in the edentulous mandible: A prospective study on Brånemark System implants over more than 20 years. Rivista Internazionale di Odontoiatria Protesica 2003;16:602–608.
25. Eskitascioglu G, Usumez A, Sevimay M, Soykan E, Unsal E. The influence of occlusal loading location on stresses transferred to implant-supported prostheses and supporting bone: A three-dimensional finite element study. J Prosthet Dent 2004; 91:144–150.
26. Fanuscu MI, Vu HV, Poncelet B. Implant biomechanics in grafted sinus: A finite element analysis. J Oral Implantol 2004; 30:59–68.
27. Holmgren EP, Seckinger RJ, Kilgren LM, Mante F. Evaluating parameters of osseointegrated dental implants using finite element analysis—A two-dimensional comparative study examining the effects of implant diameter, implant shape, and load direction. J Oral Implantol 1998;24:80–88.
28. Huiskes R, Weinans H, van Rietbergen B. The relationship between stress shielding and bone resorption around total hip stems and the effects of flexible materials. Clin Orthop Relat Res 1992;274:124–134.
29. Ugural AC. Stresses in beams. In: Corrigan JJ, Bradley JW (eds). Mechanics of Materials. Singapore: McGraw-Hill, 1991; 175–182.
30. Bolind PK, Johansson CB, Becker W, Langer L, Severtz EB Jr, Albrektsson TO. A descriptive study on retrieved nonthreaded and threaded implant designs. Clin Oral Implants Res 2005;16: 447–455.
31. Siegele D, Soltesz U. Numerical investigations of the influence of implant shape on stress distribution in the jaw bone. Int J Oral Maxillofac Implants 1989;4:333–340.
32. Huja SS, Qian H, Roberts WE, Katona TR. Effects of callus and bonding on strains in bone surrounding an implant under bending. Int J Oral Maxillofac Implants 1998;13:630–638.